

Energy & Environmental Science

Accepted Manuscript



This is an *Accepted Manuscript*, which has been through the Royal Society of Chemistry peer review process and has been accepted for publication.

Accepted Manuscripts are published online shortly after acceptance, before technical editing, formatting and proof reading. Using this free service, authors can make their results available to the community, in citable form, before we publish the edited article. We will replace this *Accepted Manuscript* with the edited and formatted *Advance Article* as soon as it is available.

You can find more information about *Accepted Manuscripts* in the [Information for Authors](#).

Please note that technical editing may introduce minor changes to the text and/or graphics, which may alter content. The journal's standard [Terms & Conditions](#) and the [Ethical guidelines](#) still apply. In no event shall the Royal Society of Chemistry be held responsible for any errors or omissions in this *Accepted Manuscript* or any consequences arising from the use of any information it contains.

High Thermoelectric Conversion Efficiency of MgAgSb-based Material with Hot-Pressed Contacts

Cite this: DOI: 10.1039/x0xx00000x

D. Kraemer,^{*a} J. Sui,^{*b,c} K. McEnaney,^a H. Zhao,^{b,d} Q. Jie,^b Z.F. Ren^{†b} and G. Chen^{†a}

Received 00th January 2012,
Accepted 00th January 2012

DOI: 10.1039/x0xx00000x

www.rsc.org/

The efficiency of heat-to-electricity conversion based on the thermoelectric effect depends on the materials' nondimensional figure of merit zT . While recent years saw an increasing number of reports of large peak zT in thermoelectric materials, efficiency data are scarce. High conversion efficiency requires not only a large average dimensionless figure of merit zT in the operational temperature range, but also good electrical and thermal contacts to the material. In this work, we experimentally demonstrate a record high thermoelectric conversion efficiency of 8.5 % with a single thermoelectric leg based on a recently reported p-type MgAgSb-based compound operating between 20 and 245 °C. The efficiency can exceed 10 % by increasing the hot side temperature to 295 °C. The sample is fabricated with silver contact pads using a one-step hot-press technique eliminating a typically required sample metallization process. This significantly simplifies the fabrication of thermoelectric elements with low electrical and thermal contact resistances.

Introduction

Thermoelectric materials can directly convert heat into electricity by imposing a temperature difference between the hot and cold junction¹⁻³. The ideal thermoelectric conversion efficiency for a material with temperature-independent properties is defined as

$$\eta = \frac{\Delta T}{T_H} \frac{\sqrt{1+zT} - 1}{\sqrt{1+zT} + \frac{T_C}{T_H}} \quad (1)$$

It is a function of ΔT as the imposed temperature difference, the hot and cold junction temperatures, T_H and T_C , respectively. The conversion efficiency is limited to a fraction of the Carnot efficiency determined by the material's dimensionless figure of merit, $zT = S^2T/\rho k$ with S , ρ , k being the Seebeck coefficient, the electrical resistivity, and the thermal conductivity, respectively. Despite their great advantages such as scalability and high power density without moving parts, thermoelectric generators have been mostly limited to niche applications due to low efficiencies. In the past decade, however, much progress has been made leading to significantly improved thermoelectric material properties that open up avenues for promising new power conversion applications⁴⁻¹⁰.

Most studies in the past report only the temperature-dependent material properties measured with commercial equipment and calculate the zT from those properties with typically rather large uncertainties^{11,12}. The emphasis usually was on the

material's peak zT which often only occurs in a narrow temperature range, however, the device efficiency is determined by the *average* material properties at the operating temperature difference and is affected by the level of the material's self-compatibility¹³. However, many challenges lie between zT and device efficiency. In addition to stable thermoelectric material properties with high average zT in the operating temperature range, good electrical and thermal contacts are essential for a thermoelectric device to live up to its expected efficiency potential¹⁴⁻¹⁶. Typically, a thin metal film is deposited onto the hot and cold junction surfaces of the thermoelectric material to act as an elemental diffusion barrier for material stability and to provide improved electrical and thermal contacts¹⁷. The deposition of the thin film metal layers increases the time and cost of the manufacturing process. In addition to the challenges in fabricating thermoelectric devices with low contact resistances, efficiency measurements are difficult due to various losses via radiative heat transfer between the device and surroundings and via heat conduction through leads attached to the device. Due to these challenges, few reports exist on experimental demonstrations of efficiencies of thermoelectric module, couple and single leg devices¹⁸⁻²⁷. Since the characterization of thermoelectric properties is prone to large uncertainties, efficiency measurements will provide confidence to property measurements.

In this work we report the single thermoelectric leg device efficiency of a recently reported p-type MgAgSb-based material which shows great potential due to its high figure of

merit with a weak temperature dependence over a rather large temperature range up to 300 °C²⁸. The sample is fabricated with silver contact pads in a three-step process which includes the ball milling of materials, a single hot-press process, and cutting the elements. No additional metallization process for the contact surfaces is required. We measure a record high efficiency of 8.5 % for the single leg device operating between 20 – 245 °C. In addition to the conversion efficiency, we simultaneously measure the material properties under the large temperature differences (*average* material properties) imposed during the efficiency measurement. From these material properties measurements we extract the temperature-dependent properties for the single leg device material to which we will refer to as *extracted* material properties²³. The obtained extracted material properties are used with the iterative method to simulate the conversion efficiency of the single leg device in the operating temperature range to support the experimental efficiency results²⁹. In order to validate the developed methods we characterize a commercial p-type bismuth telluride leg which can be used as a standard sample due to its reliable and isotropic material properties and stable contacts²³. This not only establishes trust in the experimental methods but also in the theoretical simulation results which rely on accurate temperature-dependent material properties to validate the measured conversion efficiencies. Our work demonstrates the importance of high average ZT for materials development and shows that MgAgSb-based material has excellent potential in converting low- to mid-temperature heat into electricity such as in waste heat recovery systems and solar thermoelectric generators.

Results and Discussion

The interested reader will find detailed discussions of thermoelectric sample fabrication as well as of the measurement methods and their challenges in the experimental section. Here, we only briefly discuss the measurements and their main challenges before discussing our results.

The measured single thermoelectric leg devices consist of the thermoelectric leg soldered with its electric contact pads in between a hot junction copper heater assembly and a cold junction copper electrode (Fig. 1(a)). The heater assembly supplies the hot junction heat input and the cold junction electrode is attached to a cold stage to maintain a steady-state temperature difference with the cold junction temperature at 20 °C. The measurements are performed under vacuum conditions to eliminate convection and air-conduction losses. The steady-state thermoelectric conversion efficiency at each set temperature difference is obtained from the measured electrical thermoelectric power output divided by the hot junction heat input power which is the most challenging quantity to measure accurately. Ideally the hot junction heat input power is directly obtained with the measured electrical heater power input. However, the radiative heat transfer and wire heat conduction via current, voltage, and thermocouple leads between the hot junction heater assembly and the

surrounding can significantly affect this measurement. We minimize the parasitic heat losses from the heater assembly by surrounding the single leg device with a heated radiation shield which is maintained close to the hot junction temperature and all wires attached to the heater assembly are thermally grounded to it. This ensures that most of the supplied electrical heater power corresponds to the hot junction heat input of the single leg device. However, the thermoelectric leg with an imposed temperature difference is to some extent radiatively heated by the surrounding radiation shield at hot junction temperature which affects the efficiency and material properties measurements. We correct the experimentally measured electrical heater power input for this radiative heat transfer using simulation results acquired from a single thermoelectric leg device model that takes into account the radiative heat transfer between the thermoelectric leg and its surroundings (A detailed description of the model is given in the electronic supplementary information (ESI)[‡]). Another important challenge that needs attention in particular for single thermoelectric leg device measurements is the possible large Joule heating in the lead supplying the thermoelectric current at the hot junction. Thermoelectric legs typically require large currents (> 1 A). Thus, even a small electrical resistance on the order of mΩ in the hot junction thermoelectric current lead can result in an additional heat input which affects the hot junction input power measurement and is difficult to quantify accurately. We minimize this Joule heating effect to below ~0.5 % of the electrical heater input power by choosing the diameter of the copper thermoelectric current lead accordingly. The measured thermoelectric conversion efficiency of the p-type MgAg_{0.965}Ni_{0.005}Sb_{0.99}-based single leg device reaches 8.5 % which is significantly higher at the imposed temperature difference of 225 °C compared to in literature reported efficiencies of devices based on legs with single thermoelectric materials^{18-23,25,26} (Fig. 1(b)). The high single thermoelectric leg conversion efficiency is demonstrated with a power output of 46.2 mW (power density of ~5.14 kW/m²) at a current of 1.48 A (current density of ~16.4 A/cm²). More details on single leg current and power densities are shown in figure S2 of the ESI[‡]. A single leg device with commercial p-type Bi₂Te₃-based material is characterized as a reference device using the developed methods. At temperature differences below ~140 °C the Bi₂Te₃-based leg yields a higher efficiency due to higher average ZT stemming from the significantly lower electrical resistivity (Fig. 2). However, its efficiency nearly levels off at 5.9 % at a temperature difference of 175 °C and is significantly outperformed by the MgAgSb-based device with linearly increasing efficiency due to its increasing average ZT exceeding that of the Bi₂Te₃-based leg. The measured average ZT exceeds 0.9 at the temperature difference of 225 °C and is likely to further increase up to a temperature difference of 280 °C²⁸. In the experiments the hot junction temperature is limited to 245 °C due to chosen solder with a solidus point of 252 °C. Our simulations which are in excellent agreement with the experiments show that increasing the hot junction temperature by only 50 °C to 295 °C yields an efficiency exceeding 10 %

which is similar to efficiencies reported in literature requiring almost twice the temperature difference and segmented thermoelectric legs comprising multiple thermoelectric materials^{20,24}. The large temperature difference and segmented thermoelectric legs not only make it more challenging in terms of the thermal stability of the materials and the electrical and thermal interfaces²¹ but it significantly increases the complexity of the device and the manufacturing processes, as well as difficulties in coupling heat into the device. In comparison, our single thermoelectric leg efficiency is demonstrated for a device using one thermoelectric material fabricated together with silver contact pads with one hot-press fabrication process, and operating at much lower temperature (see experimental section).

The device efficiency is simulated based on the iterative method using temperature-dependent material properties in combination with the discretized Domenicali's equations^{30,29}, and the results show excellent agreement with the experimental data. The material properties are extracted from the average

material properties measurements (direct and absolute) performed under the large steady-state set temperature differences during the single leg efficiency measurement using a previously introduced procedure²³ (Fig. 2). It is a steady-state differential method in which the material properties are related to the change in the measured parameters upon the change in the imposed steady-state temperature difference (see experimental section). All measured material properties are device properties which include possible electrical and thermal contact resistances. As expected the extracted material properties have significantly stronger temperature dependence and show a higher peak ZT compared to the average material properties. However, the average ZT at the operating temperature difference is what determines the thermoelectric device efficiency. Additionally, the level of the material's self-compatibility can also compromise the thermoelectric performance^{31,32}.

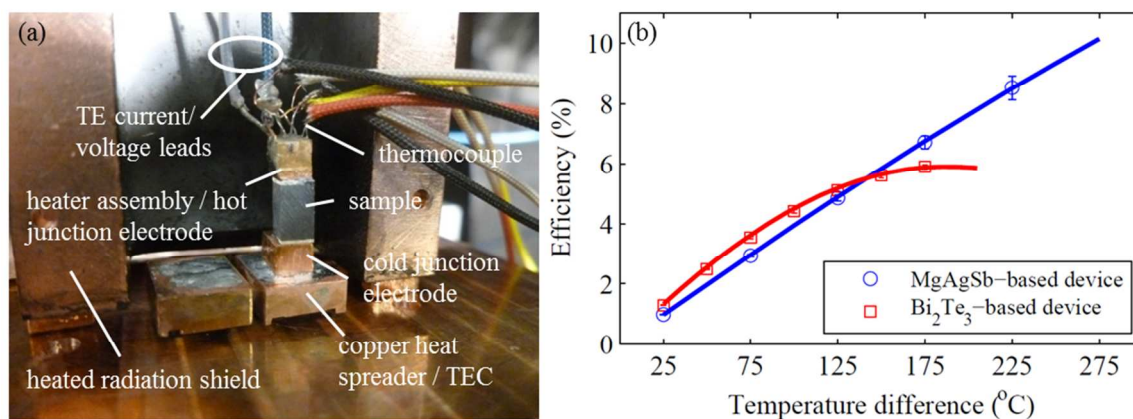


Fig. 1 Single thermoelectric leg device efficiency results for a p-type nickel-doped MgAgSb-based compound with hot-pressed silver contacts. (a) Fabricated single thermoelectric leg device with the sample soldered to the copper heater assembly (also acting as the hot junction electrode) and the copper cold junction electrode. The device is soldered onto a thermoelectric cooler (TEC) which is mounted onto a liquid cooled cold plate and surrounded by a heated radiation shield. (b) Efficiency results of a single thermoelectric leg device based on the p-type nickel-doped MgAgSb compound (blue circles) compared to a device based on a commercial p-type doped bismuth telluride sample (red squares). Solid lines correspond to simulation results obtained with the iterative method based on intrinsic material properties extracted from average material properties measurements.

The Seebeck coefficients are significantly higher for the MgAgSb-based compound over the whole temperature range compared to the Bi₂Te₃-based material (Fig. 2(a)). The Seebeck coefficients have maxima and then decrease monotonically which is caused by the thermal excitation of energy carriers resulting in a cancellation between electrons and holes with rising material temperature. The electrical resistivity values of the two materials are not only significantly different in their absolute value but also in their temperature dependence (Fig. 2(b)). The electrical resistivity monotonically increases with temperature for the Bi₂Te₃-based material which can be attributed to growing electron-phonon scattering. The electrical resistivity of the MgAgSb-based material on the other hand shows a maximum and decreases due to increased carrier

excitation. The thermal conductivities of both materials show the typical positive temperature dependence for small bandgap semiconductor materials in that temperature range due to the bipolar thermal-diffusion effect.

The single thermoelectric leg device efficiency and average material properties measurements were performed 6 times with each run requiring between 6 – 8 hrs. No significant changes in the efficiency or material properties are observed suggesting promising thermal stability of the material and of the electrical and thermal contacts. Despite the same applied hot-press process, our extracted properties for the MgAgSb-based material differ to some extent from the previously reported experimental results (ESI Fig. S4[†])²⁸. We believe the difference originates from the difference in the hot-press

conditions for the thermoelectric material due to the addition of the metal contact powder (see experimental section) which likely affects the current flow and temperature distribution within the hot press³³. This underlines the device fabrication

challenges that come with the efforts to bridge the gap between measured material properties and the demonstration of the corresponding thermoelectric conversion efficiency.

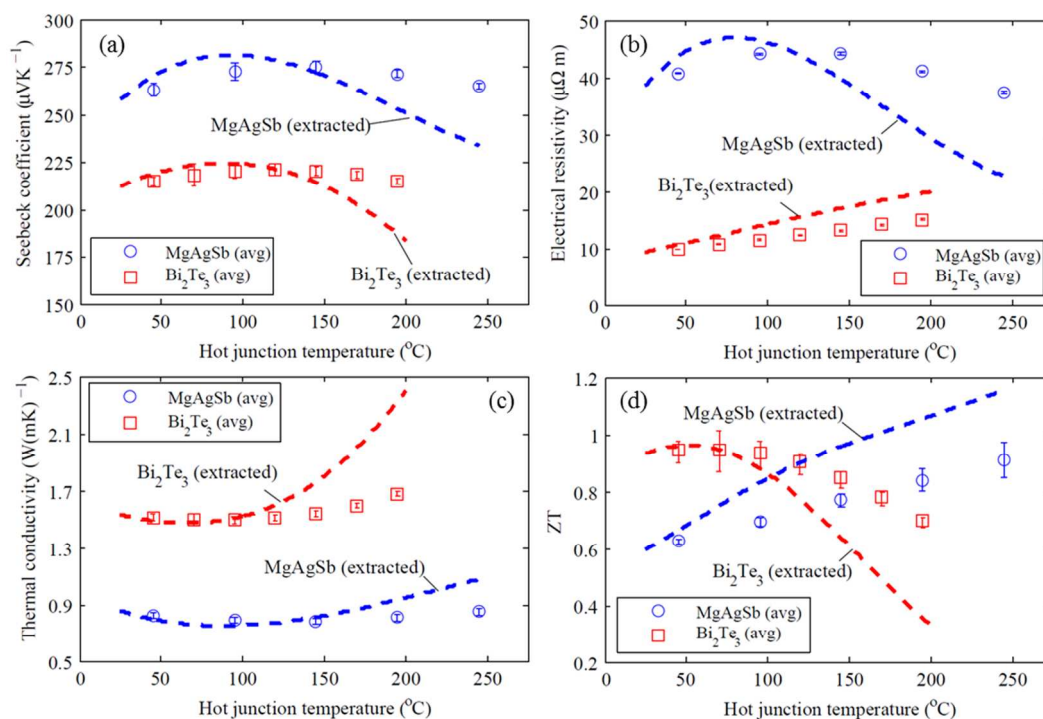


Fig. 2 Measured material properties. Properties measured under a large temperature difference (*average*) with the cold side at 25 °C during the efficiency measurement of the fabricated p-type MgAgSb-compound based device (blue circles) compared to the commercial p-type bismuth telluride based device (red squares). From these large temperature difference measurements, we *extract* the temperature-dependent material properties (dashed lines)²³. (a) Seebeck coefficient. (b) Electrical resistivity. (c) Thermal conductivity. (d) Calculated ZT.

Thus far, thermoelectric materials research has focused on increasing the material's peak ZT. However, the device efficiency is mostly determined by the *average* ZT over the imposed temperature difference. In Fig. 3, we summarize the reported maximum measured efficiency of different materials. The strategy to achieve higher thermoelectric conversion efficiencies seems to have been so far to increase the operating temperature difference. The reported measurements of thermoelectric devices based on legs with single thermoelectric materials only achieved a maximum efficiency of ~3 % at a temperature difference of 600 °C for iron disilicide and manganese silicide based materials¹⁹, ~5.5 % at a temperature difference of 400 °C for zinc antimony and constantan based materials¹⁸ and ~5.5 % at a temperature difference of ~147 °C for the same commercial bismuth telluride based material as used in this work²³. Our demonstration of a thermoelectric efficiency of 8.5 % at a relatively small temperature difference of 225 °C is a notable step forward for thermoelectric generators because similar conversion efficiencies of around 10 % have only been reported for couple devices based on skutterudite materials at more than twice the temperature difference^{20,25}. This poses a significant challenge in terms of

the material's long-term stability especially under vacuum²¹. For thermoelectric modules based on skutterudite materials efficiencies between 7 – 8 % were reported at a temperature difference from 460 °C to 550 °C^{26,27}. The highest thermoelectric generator efficiencies of 10 to 15 % have been demonstrated by imposing even larger operating temperature differences of approximately 500 to 850 °C and using segmented thermoelectric legs comprising multiple thermoelectric materials including skutterudite, lanthanum telluride and ytterbium manganese antimony based materials²⁴. Sophisticated contact metallization layers and coatings to suppress high temperature material sublimation are required for enhanced electrical and thermal contacts and long-term stability which significantly increases the complexity of the device and its fabrication process and with that its cost. However, large-scale deployment of thermoelectric generators such as in waste heat recovery systems or in solar thermoelectric generators requires simple and cost-effective thermoelectric devices with high efficiencies³⁴.

Therefore, our experimental demonstration of 8.5 % thermoelectric conversion efficiency with a MgAgSb-based compound at a relatively low temperature difference of 225 °C

in combination with a simple and low-cost fabrication process is a significant step towards large-scale deployment of thermoelectric devices as low- to mid-temperature power converters. Additionally, accurate thermoelectric efficiency measurements give great confidence in the measured temperature-dependent properties and emphasize the

importance of the *average* ZT under operating temperature difference rather than the peak zT for materials development. Further research is required to fabricate a compatible n-type thermoelectric leg with comparable performance in similar temperature range.

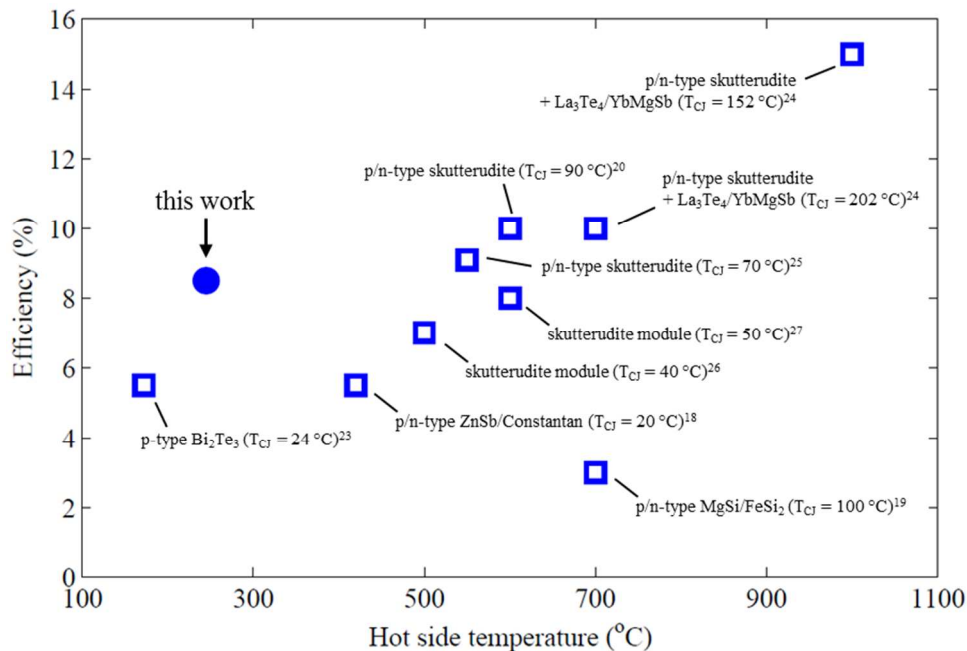


Fig. 3 Efficiency comparison. Reported maximum thermoelectric device efficiencies (open squares) as a function of hot junction temperature compared to the single leg device based on p-type MgAgSb-based material with hot-pressed metal contacts and cold junction temperature (T_{CJ}) at 20 °C (solid circle).

Experimental

Sample fabrication

The p-type $\text{MgAg}_{0.965}\text{Ni}_{0.005}\text{Sb}_{0.99}$ thermoelectric sample with silver contact pads is prepared in a three-step fabrication process. The silver powder for the contact pads is purchased from Aldrich with a particle size of 10 μm . The thermoelectric material powder is prepared according to the experimental ball milling procedure described in the previous publication²⁸. Then the thermoelectric MgAgSb-based material powder is placed between the silver contact pad powders in a hot-press (Fig. 4(a)). The materials are hot-pressed under direct current at 575 K for 8 min to form the solid sample with silver contact pads. The as-pressed disc was then annealed at 575 K in air for 30 minutes. The pressed disc is cut to smaller elements with cross-sectional area of 3 mm x 3 mm (Fig. 4(b)). The length of the thermoelectric material section is approximately 5 mm and the silver contact pads are between 0.25 and 0.35 mm thick. We choose Ag as the electrical contact pad material for the MgAgSb-based thermoelectric element not only for its high electrical and thermal conductivity but also because it is easy to solder to and because its softness permits pressing a dense Ag

contact pad together with the thermoelectric material at 300 °C. In addition to well-matched coefficients of thermal expansion with $19.5 \times 10^{-6}/^\circ\text{C}$ for Ag and $20 \times 10^{-6}/^\circ\text{C}$ for the MgAgSb-based material, silver is one of the component elements of the thermoelectric material which reduces elemental diffusion due to the smaller concentration gradient. All these attributes help creating a strong and thermally stable bond with low electrical interface resistance. Additionally, silver does not introduce other phases to the interface which also reduces the potential of deterioration of the thermoelectric properties over time. A clean and well-defined interface between the MgAgSb-based compound and the Ag contact pad suggests only minimal elemental inter-diffusion during the hot-press and annealing process (Fig. 4(c) and (d)). Even though some elemental inter-diffusion is observed after the single thermoelectric leg experiments (ESI Fig. S5[†]), no significant change in the thermoelectric leg device performance and properties including the electrical contact resistance ($< 2\%$ relative to thermoelectric leg resistance) is observed during our experimental timeframe of several days. This suggests promising thermal stability of the fabricated thermoelectric leg and supports our choice of Ag as the contact pad material. Nevertheless, other metals (Sn, Cu, Al) have been tried as

potential contact pad candidates without much success due to detrimentally large electrical contact resistance. However, while it is beyond the scope of this work, a more detailed study of the long-term thermal stability of the interface region between the thermoelectric material and the hot-pressed contact pad could be subject of future research.

Even though we demonstrate the technique for a ball-milled thermoelectric material powder, the technique can also be applied to single crystals. However, it will require cutting the single crystal sample to the necessary disc dimensions to fit the hot press. The contact pad material powder sandwiching the single crystal can then be hot-pressed to react with the thermoelectric material and form a dense contact pad with low resistance and high mechanical strength.

liquidus point of 260 °C permits a soldering process below the hot-press temperature to prevent changes in the properties of the MgAgSb-based material. The heater assembly uses a thin film resistance temperature detector (RTD – PT100) as the electrical heater element brazed ($\text{Ag}_{56}\text{Cu}_{22}\text{Zn}_{17}\text{Sn}_5$) into a small copper block of same cross-sectional area as the thermoelectric leg to minimize radiative thermal shunting between the heater assembly and the cold side. The hot junction current and voltage leads for the device and the bead of a 125 μm K-type thermocouple are embedded in the copper heater assembly. The device is soldered to a temperature controllable cold stage consisting of a copper heat spreader on top of a thermoelectric cooler module (TEC) which is soldered to a liquid cooled cold plate. The cold junction thermoelectric current and voltage leads as well as a 125 μm K-type thermocouple are embedded in the copper heat spreader. The single leg device is surrounded by a heated radiation shield which is suspended on ceramic pillars. Its temperature is measured with a 125 μm K-type thermocouple.

The single leg device efficiency is measured in a vacuum chamber at a pressure below 10^{-4} mbar by performing thermoelectric current (I_{TE}) – voltage (V_{TE}) measurements at various steady-state set temperature differences imposed across the device with the cold junction temperature, T_{CJ} , maintained at 20 °C. The hot junction temperature, T_{HJ} , is maintained at a constant value during the $I_{\text{TE}}-V_{\text{TE}}$ curve measurement by accordingly adjusting the hot junction electrical heater power input, P_{H} for each set current flowing through the device. When the system reaches a steady state the measurement parameters I_{TE} , V_{TE} , P_{H} , T_{HJ} , T_{CJ} , and the radiation shield temperature, T_{RS} are recorded.

The single thermoelectric leg efficiency is calculated for each current and temperature difference setting with

$$\eta_{\text{TE}}(I_{\text{TE}}) = \frac{P_{\text{TE}}}{Q_{\text{HJ}}} \approx \frac{P_{\text{TE}}}{P_{\text{H}}} \quad (2)$$

where P_{TE} is the thermoelectric leg power output $P_{\text{TE}} = I_{\text{TE}}V_{\text{TE}}$ and Q_{HJ} is the hot junction heat input. This heat input is equal to the electrical heater input power, $P_{\text{H}} = I_{\text{H}}V_{\text{H}}$ with I_{H} and V_{H} as the supplied heater current and measured voltage, respectively, if the parasitic heat losses such as the radiative heat transfer and wire heat conduction from the heater assembly to the surroundings are negligible. The maximum thermoelectric efficiency at each temperature difference is obtained from the 4th order polynomial fit of the η_{TE} vs I_{TE} curve as described in the ESI in more detail[†].

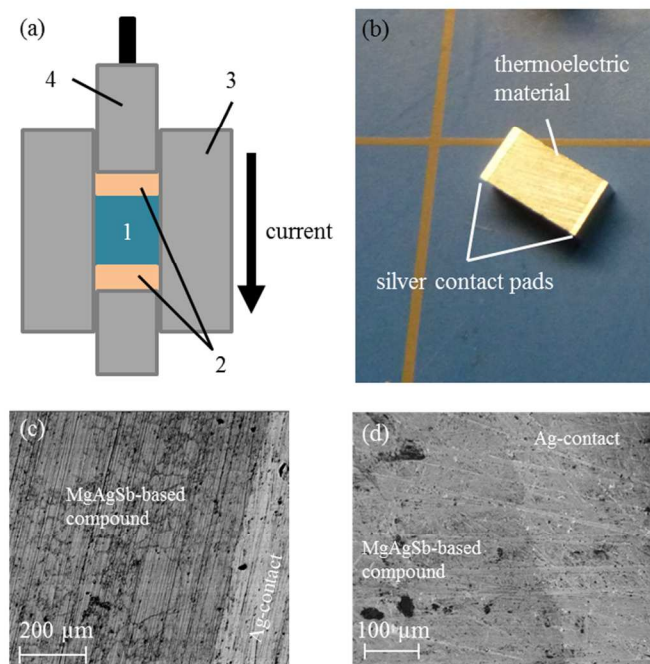


Fig. 4 Thermoelectric sample fabrication with electrical contact pads using hot-press technique. (a) Thermoelectric material powder (1) is sandwiched between electrical contact pad material (2) inside the graphite die (3) of the hot-press. While graphite piston (4) applies pressure with current flowing through piston, die, and materials increases the hot-press temperature. (b) P-type $\text{MgAg}_{0.965}\text{Ni}_{0.005}\text{Sb}_{0.99}$ sample (3 mm x 3 mm x 5 mm) as fabricated with a three-step process (ball milling, hot-pressing, cutting) with silver contact pads with thickness of $\sim 0.25 - 0.35$ mm on each end. SEM pictures with magnification of 100X (c) and 395X (d) show a clean and well-defined interface between the MgAgSb-based compound and the Ag contact pad after the hot-press and annealing process.

Experimental setups and measurement methods

The single leg device consists of the thermoelectric leg soldered ($\text{Pb}_{90}\text{Sb}_{10}$ – solidus: 252°C / liquidus: 260°C) between a hot junction heater assembly and a cold junction electrode (Fig. 1(a) and Fig. 5). The chosen solder creates a mechanically strong solder joint with low electrical contact resistance between the silver and copper surfaces and its

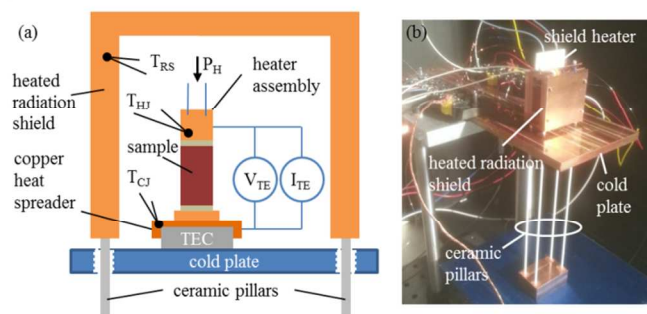


Fig. 5 Experimental setup to conduct single thermoelectric leg device efficiency and material properties measurements under large temperature differences. (a) The efficiency measurement is performed under vacuum with a suspended (ceramic pillars) heated copper radiation shield at temperature T_{RS} surrounding the single leg device and maintained close to the heater assembly temperature, T_{HJ} . The device consisted of the thermoelectric sample soldered between a copper cold junction electrode and a copper heater assembly which also functions as the hot junction electrode. The device is soldered to the copper heat spreader of a temperature controllable cold stage which consists of liquid cooled cold plate with a thermoelectric module (TEC) soldered to it for accurate control of the cold junction temperature, T_{CJ} . K-type thermocouples embedded in the heater assembly, the copper heat spreader and the radiation shield are used as temperature sensors. In order to control the hot junction temperature the electrical heater power input, P_H can be adjusted. The leads for the thermoelectric current, I_{TE} , and the voltage, V_{TE} , measurement are embedded in the heater assembly and the cold stage copper heat spreader. (b) Experimental setup inside vacuum chamber. Radiation shield is suspended on ceramic pillars and completely surrounds the single thermoelectric leg device.

Instead of calibrating for the parasitic heat losses which can significantly reduce the signal-to-noise ratio of the experiment, we minimize the parasitic heat losses from the heater assembly by maintaining the heated radiation shield close to the heater assembly temperature. However, as a consequence there is an additional radiative heat input from the radiation shield to the thermoelectric leg which needs to be corrected for to obtain the actual single thermoelectric leg efficiency.

Radiation correction

We correct for the aforementioned radiation contribution by estimating the effect of the radiative heat transfer between the leg and the surrounding heated radiation shield on the efficiency measurement using simulation results obtained from the temperature-dependent material properties with the iterative method²⁹. The equations used are modified to include the radiative heat transfer between the thermoelectric leg with an effective IR emittance and its surroundings which is assumed to be a blackbody at hot junction temperature³⁵. For more details the model is described in the ESI[†]. The IR emittance is estimated with following procedure. We perform an additional experiment to measure the average thermal conductivity with a modified setup (Fig. 6). The only difference to the experimental setup used for the single leg device efficiency and average properties measurements is the addition of a copper radiation shield which is thermally grounded to the cold junction copper electrode and tightly surrounds the thermoelectric leg with a gap of approximately 0.1 – 0.3 mm (Fig. 6(a) and (b)). Consequently, the effect of the leg radiation on the thermal conductivity measurement is minimized in this

experiment. To match those measurement results, the average thermal conductivity data measured during the single leg device efficiency experiments (without tight copper radiation shield) requires a radiation correction using an effective IR emittance of 0.4 (Fig. 6(c)). The error bars include the error in the measured temperature difference from the statistical and systematic thermocouple measurement uncertainties and the statistical and systematic error from the hot junction power input measurement using an uncertainty in the IR emittance of ± 0.2 . The IR emittance of 0.4 ± 0.2 is also used for the radiation correction calculation of the single thermoelectric leg efficiency data.

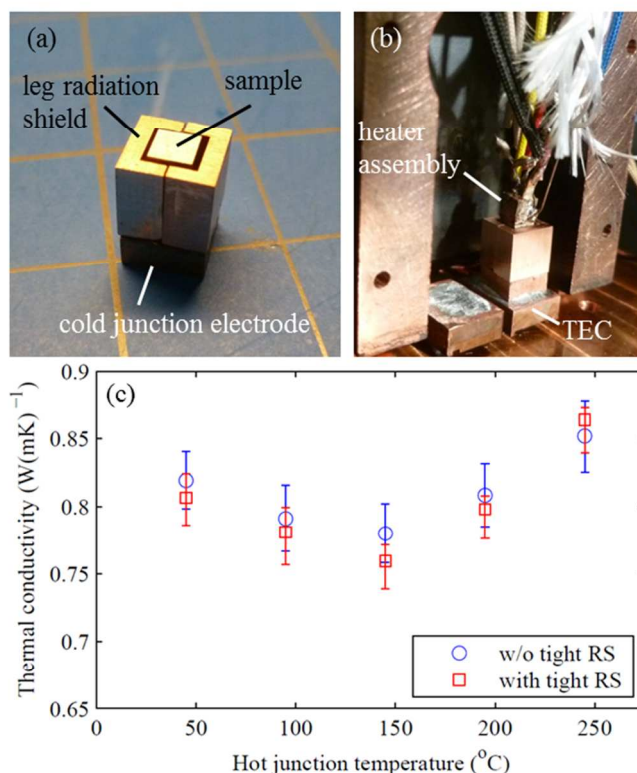


Fig. 6 Measurements of the average thermal conductivity of the thermoelectric leg under large temperature using a modified setup with an additional copper radiation shield. (a) Copper radiation shield tightly surrounds the thermoelectric leg sample (gaps are $\sim 0.1 - 0.3$ mm) and is thermally grounded to the cold junction electrode. (b) For the efficiency measurement, the sample is soldered between the hot junction heater assembly and the cold junction electrode. The device surrounded by the tight copper radiation shield is soldered onto the cold stage. The system is surrounded by the heated copper radiation shield maintained close to the heater assembly temperature. (c) Measured average thermal conductivity results (red squares) are in good agreement with average thermal conductivity results (corrected for leg radiation effect using an effective emittance of 0.4) obtained during the efficiency experiment without tight radiation shield (blue circles).

Average and extracted material properties measurements

The temperature-dependent material properties are *extracted* from the *average* material properties measurements at large

temperature differences during the efficiency experiment using a previously established method²³. The average Seebeck coefficient and thermal conductivity are obtained at open circuit conditions by measuring the Seebeck voltage, V_S , and the electrical heater input power, P_H , respectively, and dividing the measured values by the measured temperature difference, $\Delta T = T_{HJ} - T_{CJ}$. The average electrical resistivity is measured with a 4-probe square-wave AC resistance method³¹. During all measurements the cold junction of the single leg device is maintained at a constant temperature of 20 °C. The extracted temperature-dependent Seebeck coefficient and thermal conductivity values are obtained from the slopes of the best polynomial fits through the V_S vs. ΔT and P_H vs. ΔT curves, respectively. The extracted electrical resistivity at T_{HJ} is calculated with $\rho(T_{HJ}) = \left(P_H \frac{dR_{avg}}{d\Delta T} + R_{avg} \frac{dP_H}{d\Delta T} \right) k(T_{HJ})^{-1}$ with R_{avg} being the measured average electrical resistance at $\Delta T = T_{HJ} - T_{CJ}$, $dR_{avg}/d\Delta T$ is the change in the average electrical resistance at T_{HJ} obtained from the slope of the best polynomial fit through the R_{avg} vs. ΔT curve, $dP_H/d\Delta T$ is the change in electrical heater power input at T_{HJ} with varying temperature difference, and $k(T_{HJ})$ is the extracted thermal conductivity.

Tests for electrical contact resistances are performed before and after the measurements at room temperature using a modified 4-probe square-wave AC resistance method with one moving voltage probe^{2,36,23}. The combined electrical contact resistance of both ends of the fabricated thermoelectric leg sample is found to be below 2 % relative to the total electrical leg resistance of approximately 19 mΩ at room temperature. The electrical contact resistances at the hot and cold junction of the single leg device include the resistances of the solder interface between copper electrode and silver contact pad, the silver contact pad itself, and of the sintered interface between the silver contact pad and the thermoelectric material created during the hot-press fabrication process.

Validation of the material properties extraction method

The accuracy of the temperature-dependent material properties is crucial for trustworthy simulations such as for the results shown in Fig. 1(b). Absolute steady-state Seebeck coefficient and thermal conductivity measurements are prone to large

uncertainties due to the introduced error from the temperature difference measurements using thermocouples. However, the thermocouple uncertainties are largely minimized by extracting the temperature-dependent Seebeck coefficient and thermal conductivity from the change in the measured Seebeck voltage and heater input power, respectively, with changing temperature difference^{31,37}. Additionally, experimental errors are reduced by measuring all material properties on the same sample in the same crystallographic directions eliminating the uncertainties from varying properties between samples and from properties anisotropies. In order to validate the used method to extract the temperature-dependent material properties from parameters measured under large temperature differences we conduct direct material properties measurements under small temperature differences on a commercial p-type bismuth telluride based material sample from the same batch using previously established high-accuracy differential methods^{31,37} (Fig. 7). We further compare the data with results obtained with commercial equipment (ZEM 3 and LaserFlash). The commercial p-type bismuth telluride material is suitable to be used as a standard material due to its reliable and isotropic material properties and stable contacts^{23,38}. The contact surfaces of the commercial samples are metallized with an additionally metallization step which likely has only a minimal effect on the sample's material properties. Overall the properties results of all the methods are in good agreement with the extracted material properties data. However, some deviation is expected because the measurements are performed on three different samples. In particular the Seebeck coefficients and electrical resistivity values show a maximum discrepancy of 5 % which can mostly be attributed to differences in the properties of the 3 samples measured (Fig. 7(a) and (b)). The measured thermal conductivities are in excellent agreement showing a deviation only at low hot junction temperatures with the reason being the uncertainty in the data fitting around the data set boundaries of the properties extraction method (Fig. 7(c)). Nevertheless, overall the data comparison gives great confidence in the extracted temperature-dependent material properties, thus in the simulation results.

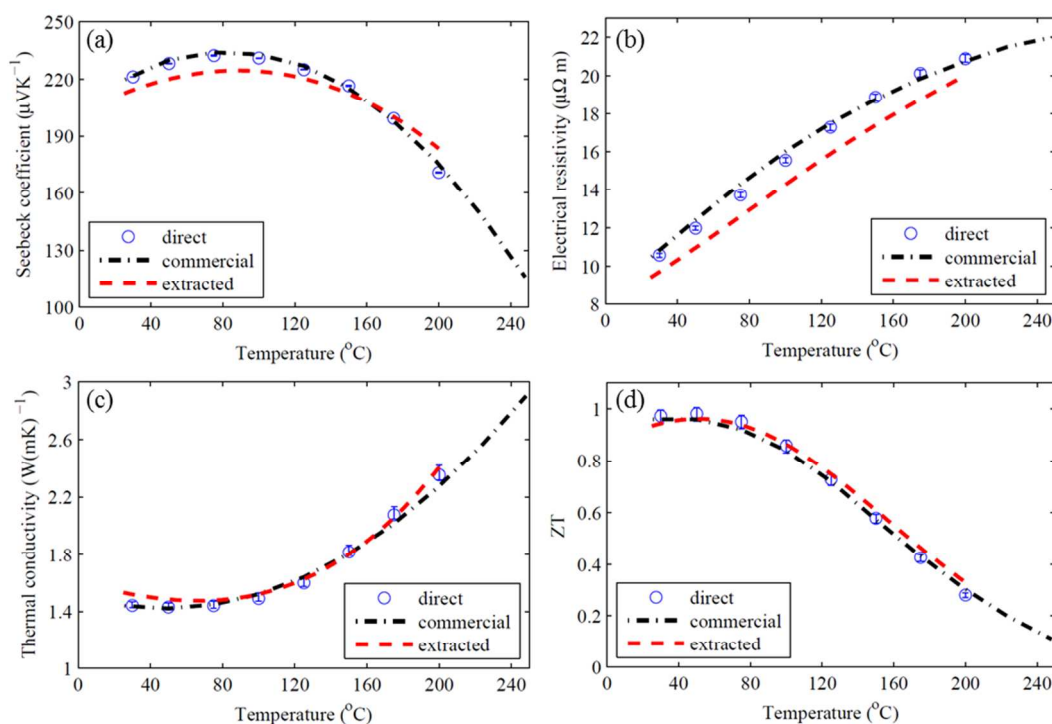


Fig. 7 Comparison of *extracted* and directly measured material properties of commercial p-type bismuth telluride. Material properties extracted from average material properties measurements during the efficiency experiments (red dashed line) are in good agreement with directly measured temperature-dependent material properties under small temperature differences using previously established high-accuracy measurement methods (blue circles)^{31,37} and commercial equipment (ZEM 3 and Laser Flash) (black dash-dotted line). (a) Seebeck coefficient. (b) Electrical resistivity. (c) Thermal conductivity. (d) Figure of merit, ZT.

Minimization of experimental uncertainties

In order to perform the single thermoelectric leg efficiency and material properties measurements with high accuracy a number of important experimental provisions require attention. For accurate temperature measurements the K-type thermocouples used are calibrated with a thermistor to an accuracy of ± 0.2 °C up to a temperature of 50 °C and above 50 °C have the manufacturer uncertainty of the larger of ± 1.1 °C or $\pm 0.004 \cdot T_{\text{reading}}$ (°C) (special limits of error). The thermocouples are brazed into the hot junction copper heater assembly and cold junction copper heat spreader in order to minimize the thermal contact resistance. Additionally, the thermocouple wires at the hot junction are thermally grounded to the heated radiation shield to minimize the heat conducted through the thermocouple bead. The current to the single leg device and to the hot junction heater is supplied by high accuracy Keithley power supplies (Model 2425) with μA resolution and the respective voltages are measured with separate voltage leads with a high accuracy digital multimeter (DMM) from Keithley (Model 2010 with scanner card) with nV resolution. The cold junctions of the thermocouples are thermally grounded to the vacuum chamber walls to ensure negligible temperature gradients. The chamber wall temperature is measured with an RTD calibrated with a thermistor to an accuracy of ± 0.2 °C and is used as the cold junction compensation. The DMM is used to conduct the wall temperature RTD measurements as well as

all thermocouple readings. The experiment is controlled using LabVIEW to ensure accurate data recording when the system reaches steady state. In order to minimize the parasitic heat losses from the hot junction heater assembly its wires are thermally grounded to the heated radiation shield which is maintained close to the hot junction temperature ($T_{\text{RS}} \approx T_{\text{HJ}}$) and has graphite coated interior walls to minimize thermal radiative shunting from the heater assembly to the cold side. One major challenge of single leg efficiency measurements is that the thermoelectric current is supplied at the hot junction. The large thermoelectric currents required for the efficiency measurement can result in significant Joule heating in the current carrying lead affecting the hot junction heat input power measurement. Thus, the diameter of the current carrying wire is chosen large enough to minimize this effect.

The error bars of the single thermoelectric leg efficiency measurement (Fig. 1) include the error from leg radiation correction introduced by the leg surface emittance uncertainty of ± 0.2 and the statistical error in the hot junction heater power input measurement. We also add a systematic error for possible Joule heating in the thermoelectric current carrying hot junction lead. The error bars for the average material properties measurements (Fig. 2) include the statistical errors from voltage and current measurements. Additionally, in the case of the Seebeck coefficient and thermal conductivity measurement they also include the statistical and systematic uncertainties from the temperature measurements.

Conclusions

We experimentally demonstrate a record high conversion efficiency of 8.5 % on a single thermoelectric leg device operating between 20 °C and 245 °C. The device is fabricated with hot-pressed silver contact pads from a recently reported MgAgSb-based material which significantly simplifies the manufacturing process of such thermoelectric legs with low contact resistances. The single leg device experiment was performed for several days showing no changes in material properties and device performance suggesting promising thermal stability. The fabricated single thermoelectric leg with hot-pressed metal contact pads can achieve 10 % at a temperature difference of 275 °C which previously has only been reported at almost twice the temperature difference and can require thermoelectric generators with segmented legs. The demonstration of comparable thermoelectric conversion efficiencies at a significantly lower operating temperature difference in combination with a simple manufacturing process represents a significant step towards large-scale deployment of thermoelectric devices as low- to mid-temperature power converters.

In the process of characterizing the device, we developed an experimental technique to measure the conversion efficiency and the average material properties of a single thermoelectric leg device at operating temperature difference. The temperature-dependent material properties are extracted from the measurements and used to simulate the theoretical conversion efficiency which supports the efficiency measurement results. Despite the challenges that come with performing an accurate thermoelectric efficiency experiment, the methods we developed and cross-checking give confidence in measured material properties which typically are prone to large uncertainties. Our work also emphasizes the importance of the average ZT in addition to the peak zT for materials research.

Acknowledgements

The authors would like to thank Dr. Bed Poudel for providing the ZEM 3 and LaserFlash measurement data of the commercial Bi₂Te₃ material and Pietro Sambegoro for the help with taking the SEM pictures. This work was partially funded by 'Solid State Solar-Thermal Energy Conversion Center (S³TEC)', an Energy Frontier Research Center funded by the US Department of Energy, Office of Science, Office of Basic Energy Sciences under Award Number: DE-SC0001299/DE-FG02-09ER46577 (for method development) and by DOE EERE under Award number: DE-EE0005806 (for thermoelectric material characterization).

Notes and references

^a Department of Mechanical Engineering, Massachusetts Institute of Technology, Cambridge, MA 02139, USA.

^b Department of Physics and TeSUH, University of Houston, Houston, TX 77204, USA.

^c National Key Laboratory for Precision Hot Processing of Metals and School of Materials Science and Engineering, Harbin Institute of Technology, Harbin 150001, China.

^d Institute of Physics, The Chinese Academy of Sciences, Beijing, 100190, China.

* Authors contributed equally.

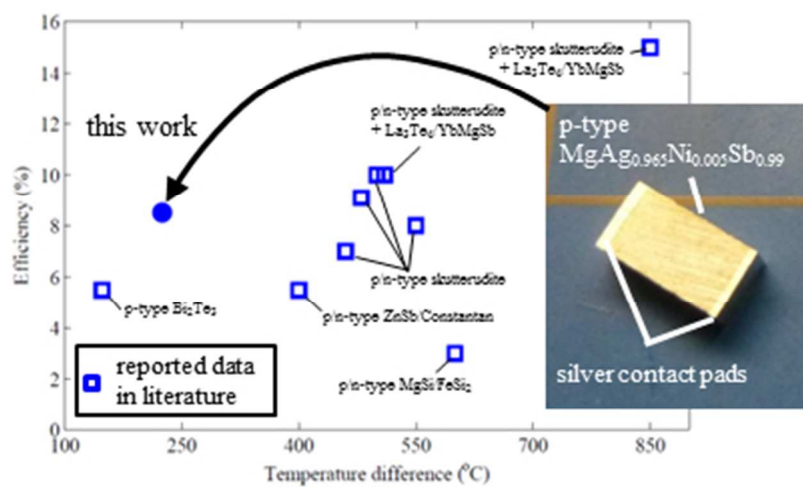
† Correspondence should be addressed to G.C. (email: gchen2@mit.edu) or to Z.F.R. (email: zren@uh.edu)

‡ Electronic Supplementary Information (ESI) available: Description of the model used for theoretical thermoelectric efficiency predictions and for the estimations of radiation corrections. Comparison of previously published and the here reported temperature-dependent material properties data. See DOI: 10.1039/b000000x/

Author contributions: D.K. developed methods and experimental setups, fabricated single leg devices, performed experiments, device modeling and simulations, analyzed data and prepared manuscript. J.S. fabricated MgAgSb-based thermoelectric elements and contributed to manuscript preparation. K.M. assisted with experiments development, performed ideal thermoelectric efficiency simulations and supported manuscript preparation. H.Z. and Q.J. assisted with sample fabrication. Z.F.R. assisted with manuscript preparation and directed research at UH. G.C. assisted with manuscript preparation and directed research at MIT.

- 1 A. F. Ioffe, *Semiconductor Thermoelements and thermoelectric cooling*, Infosearch Ltd., 1957.
- 2 H. J. Goldsmid, *Electronic Refrigeration*, Plenum Press, 1964.
- 3 D. M. Rowe, *Thermoelectrics Handbook: Macro to Nano*, Taylor & Francis Group, LLC, 2006.
- 4 J. R. Sootsman, D. Y. Chung and M. G. Kanatzidis, *Angew. Chem., Int. Ed. Engl.*, 2009, **48**, 8616–8639.
- 5 M. S. Dresselhaus, G. Chen, M. Y. Tang, R. G. Yang, H. Lee, D. Z. Wang, Z. F. Ren, J.-P. Fleurial and P. Gogna, *Adv. Mater.*, 2007, **19**, 1043–1053.
- 6 G. J. Snyder and E. S. Toberer, *Nat. Mater.*, 2008, **7**, 105–114.
- 7 M. Zebarjadi, K. Esfarjani, M. S. Dresselhaus, Z. F. Ren and G. Chen, *Energy Environ. Sci.*, 2012, **5**, 5147–5162.
- 8 D. Kraemer, B. Poudel, H.-P. Feng, J. C. Caylor, B. Yu, X. Yan, Y. Ma, X. Wang, D. Wang, A. J. Muto, K. McEnaney, M. Chiesa, Z. F. Ren and G. Chen, *Nat. Mater.*, 2011, **10**, 532–538.
- 9 L. E. Bell, *Science*, 2008, **321**, 1457–1461.
- 10 D. M. Rowe, *Thermoelectrics and its Energy Harvesting: Modules, Systems, and Applications in Thermoelectrics*, Taylor & Francis Group, LLC, 2012.
- 11 H. Wang, *International Round-Robin on Transport Properties of Bismuth Telluride*, 1–19, 2011.
- 12 H. Wang, W. D. Porter, H. Böttner, J. König, L. Chen, S. Bai, T. M. Tritt, A. Mayolet, J. Senawiratne, C. Smith, F. Harris, P. Gilbert, J. Sharp, J. Lo, H. Kleinke and L. Kiss, *J. Electron. Mater.*, 2013, **42**, 1073–1084.
- 13 G. J. Snyder and T. Ursell, *Phys. Rev. Lett.*, 2003, **91**, 148301.
- 14 M. H. Cobble, Ch. 39 in *CRC Handb. Thermoelectr.* (D. M. Rowe), Taylor & Francis Group, LLC, 1995.
- 15 D. M. Rowe and G. Min, *IEE Proceedings - Sci. Meas. Technol.*, 1996, **143**, 351–356.
- 16 D. M. Rowe and G. Min, *J. Power Sources*, 1998, **73**, 193–

- 198.
- 17 Y. M. Belov, S. M. Maniakin and I. V. Morgunov, Ch. 20 in *Thermoelectr. Handb. Macro to Nano* (D. M. Rowe), Taylor & Francis Group, LLC, 2006.
- 18 M. Telkes, *J. Appl. Phys.*, 1954, **25**, 765.
- 19 E. Gross, M. Riffel and U. Stoehrer, *J. Mater. Res.*, 1995, **10**, 34–40.
- 20 T. Caillat, J.-P. Fleurial, G. J. Snyder and A. Borshchevsky, in *Proceedings of 20th Int. Conf. on Thermoelectrics*, (Cat. No.01TH8589), 282–285, 2001.
- 21 El-genk, M. S., Saber, H. H., Sakamoto, J., Caillat, T., in *Proceedings of 22nd Int. Conf. on Thermoelectrics*. 417–420, 2003.
- 22 J.-P. Fleurial, K. Johnson, J. Mondt, J. Sakamoto, G. J. Snyder, C.-K. Huang, R. Blair, G. Stapfer, T. Caillat, W. Determan, P. Frye, B. Heshmatpour, M. Brooks and K. Tuttle, in *IEEE Proceedings of Aerosp. Conf.*, 2006.
- 23 A. J. Muto, D. Kraemer, Q. Hao, Z. F. Ren and G. Chen, *Rev. Sci. Instrum.*, 2009, **80**, 093901.
- 24 T. Caillat, S. Firdosy, B. Cheng, J. Paik, J. Chase, T. Arakelian, L. Lara, J.-P. Fleurial, in *Proceedings of Nucl. Emerg. Technol. Space*, 2012.
- 25 A. J. Muto, J. Yang, B. Poudel, Z. F. Ren and G. Chen, *Adv. Energy Mater.*, 2013, **3**, 245–251.
- 26 J. R. Salvador, J. Y. Cho, Z. Ye, J. E. Moczygemba, A. J. Thompson, J. W. Sharp, J. D. Koenig, R. Maloney, T. Thompson, J. Sakamoto, H. Wang, A. A. Wereszczak, *Phys. Chem. Chem. Phys.*, 2014, **16**, 12510–20.
- 27 J. Q. Guo, H. Y. Geng, T. Ochi, S. Suzuki, M. Kikuchi, Y. Yamaguchi, S. Ito, *J. Electron. Mater.*, 2012, **41**, 1036–1042.
- 28 H. Zhao, J. Sui, Z. Tang, Y. Lan, Q. Jie, D. Kraemer, K. McEnaney, A. Guloy, G. Chen, Z. F. Ren, *Nano Energy*, 2014, **7**, 97–103.
- 29 T. P. Hogan, Ch. 12 in *Thermoelectr. Handb. Macro to Nano* (D. M. Rowe), Taylor & Francis Group, LLC, 2006.
- 30 C. A. Domenicali, *Phys. Rev.*, 1953, **92**, 877–881.
- 31 D. Kraemer and G. Chen, *Rev. Sci. Instrum.*, 2014, **85**, 045107.
- 32 G. J. Snyder, *Appl. Phys. Lett.*, 2004, **84**, 2436.
- 33 A. J. Muto, G. Chen, A. Sufisor and E. Hardt, *Thermoelectric Device Characterization and Solar Thermoelectric System Modeling*, 2011.
- 34 S. K. Yee, S. LeBlanc, K. E. Goodson and C. Dames, *Energy Environ. Sci.*, 2013, **6**, 2561.
- 35 D. Kraemer, K. McEnaney, M. Chiesa and G. Chen, *Sol. Energy*, 2012, **86**, 1338–1350.
- 36 R. J. Buist and S. J. Roman, in *Proceedings of 18th Int. Conf. Thermoelectrics*, 249–251, 1999.
- 37 D. Kraemer and G. Chen, *Rev. Sci. Instrum.*, 2014, **85**, 025108.
- 38 B. Poudel, Q. Hao, Y. Ma, Y. Lan, A. Minnich, B. Yu, X. Yan, D. Wang, A. J. Muto, D. Vashaee, X. Chen, J. Liu, M. S. Dresselhaus, G. Chen, Z. F. Ren, *Science*, 2008, **320**, 634–8.



High conversion efficiency is demonstrated at a relatively small temperature difference for a MgAgSb-based single thermoelectric leg with hot-pressed contacts.
73x45mm (150 x 150 DPI)

Broader context box:

Thus far, thermoelectric materials research has focused on increasing the material's peak zT . However, the device efficiency is mostly determined by the average ZT over the imposed temperature difference. In this work, we experimentally demonstrate a record high thermoelectric conversion efficiency of 8.5 % with a single thermoelectric leg based on a recently reported p-type MgAgSb-based compound operating between 20 and 245 °C. Similar efficiencies have only been demonstrated at twice the temperature difference with hot side temperatures beyond 500 °C. In addition, the sample is fabricated with silver contact pads using a one-step hot-press technique eliminating a typically required sample metallization process. This significantly simplifies the fabrication of thermoelectric elements with low electrical and thermal contact resistances. We believe that our demonstration of a record high conversion efficiency at a relatively low temperature difference of 225 °C in combination with a simple and low-cost fabrication process is a significant step towards large-scale deployment of thermoelectric devices as low- to mid-temperature power converters. Additionally, accurate thermoelectric efficiency measurements give great confidence in the measured temperature-dependent properties, the real-world materials' applicability and emphasize the importance of the *average* ZT under operating temperature difference rather than the peak zT for materials development.